Optimisation of a crystal design for a Bonse-Hart camera

Mario Villa,[a*] Matthias Baron,[a,b] Martin Hainbuchner,[a] Erwin Jericha,[a] Vincent Leiner,[b] Dietmar Schwahn,[c] Erwin Seidl,[a] Jochen Stahn[d] and Helmut Rauch [a]

[a]Atominstitut, Stadionallee 2, A-1020 Wien, Austria, [b]Institut Laue-Langevin, F-38042 Grenoble, France, [c]Forschungszentrum Jülich GmbH, D-52425 Jülich, Germany, and [d]Paul Scherrer Institut, CH-5234 Villigen, Switzerland. E-mail: mvilla@ati.ac.at

Bonse-Hart double-crystal diffractometers (DCDs) with multi-bounce channel-cut crystals show rocking curves that depart dramatically from dynamical diffraction theory in their wings. The intrinsic background is many orders of magnitude higher than the predictions of dynamical diffraction theory. This effect was studied at the ultra-small-angle neutron scattering facility at the Atominstitut in Wien and at facilities in Grenoble, Jülich and Villigen. The scattering intensity contains Bragg reflections from the front and the back faces, and thermal diffuse scattering from the internal volume. The aim of this study was to eliminate this contamination and develop a new crystal design which provides optimal resolution. Therefore different ways were tested. In the first step the contamination was eliminated by cutting a groove in the middle of the back plate of the channel-cut crystals and inserting a cadmium absorber in this groove. With this modification an additional suppression of the wings of the rocking curve of about one order of magnitude was achieved. After this, we developed a new design for a DCD. The concept for this new crystal design was to avoid the back reflection and the thermal diffuse scattering. The different steps on the way to produce these crystals are presented in a detailed way. The crystal preparation and the different instruments where these crystals have been tested are also described.

Keywords: double crystal diffractometers , dynamical diffraction theory, USANS, Bragg reflection

1. Introduction

To describe diffraction phenomena of neutrons by a perfect crystal, the Bragg law alone is not adequate. To understand the relationship between the incoming neutrons and the periodic crystal dynamical diffraction theory is needed (Rauch & Petrascheck, 1978; Zachariasen, 1967). In this dynamical theory there are two cases, the Bragg case and the Darwin case. The simple relation between these two cases was studied by Takahasi & Hashimoto (1995). There theoretical and experimental studies was one of the main reasons to develop a new crystal design. The second main motivation was the work of Agamalian and his group during the last years (Agamalian, Wignall & Triolo, 1997; Agamalian *et al.*, 1998). The Bonse-Hart double crystal diffractometer (DCD) (Bonse & Hart, 1965) is now used in many research laboratories around the world. One of the main problems of this technique is the user community. Compared to small-angle neutron scattering (SANS), which is a major tool for studies in different fields, DCDs for ultra-small-angle neutron scattering (USANS) are not so established. To open the USANS DCD to the large community of SANS users, it is important to optimise the signal-to-background ratio and to increase the Q-range of the instrument (Q is the modulus of the scattering vector, $4\pi\sin\theta/\lambda$ where θ is half the scattering angle and λ the wavelength of the incident neutrons). This work was performed under cooperation between different neutron sources around Europe. The first steps were done in Wien, additional experiments were performed in Jülich, Villigen and at the ILL.

2. Theoretical background

The rocking curve for a DCD with channel-cut crystals is a convolution of reflectivity curves from the monochromator and the analyser crystal

$$I(\Delta)=\int R_1(y)^n\,R_2(y+\Delta)^m\,dy \qquad (1)$$

where n and m are the numbers of reflections in the monochromator and the analyser crystal. The reflectivity $R(y)$ is described either by the Darwin formula (Darwin, 1914) or by the Ewald formula (Ewald, 1917). The Darwin formula is expressed as

$$R_{\rm D}(y)=\frac{P_{\rm G}}{P_{\rm e}}=\begin{cases}1 & |y|\le 1\\ \left[\,|y|-\sqrt{(y^2-1)}\,\right]^2 & |y|>1\end{cases} \qquad (2)$$

in the case of non absorbing crystals. The dimensionless angular parameter y describes the deviation of the incident beam from the Bragg condition corrected for the refraction effect. In the region of $y \le 1$ total reflection occurs. In contrast, the Ewald formula is described as

$$R_{\rm E}(y)=\frac{P_{\rm G}}{P_{\rm e}}=\begin{cases}1 & |y|\le 1\\ 1-\sqrt{1-\dfrac{1}{y^2}}. & |y|>1\end{cases} \qquad (3)$$

The difference between these two cases is shown in Fig. 1.

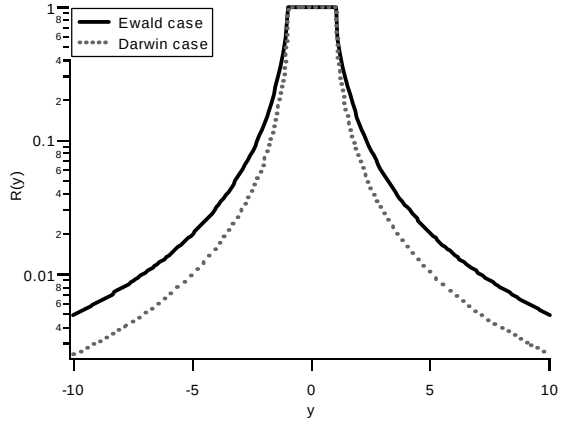

Figure 1

Comparison of the Ewald and the Darwin cases.

The profiles of these two curves differ considerably in their tail parts, and the Ewald formula gives twice the value of the Darwin formula at their tails. Takahashi & Hashimoto (1995) have shown that for a transparent thick crystal, the Darwin formula gives the reflectivity only from the front side, while the Ewald equation describes the total Bragg reflection from the front and the back.

3. Optimisation of the crystal design

To understand the difference of the Ewald and the Darwin case, and therefore to optimise the crystal design for a DCD, different steps to produce crystals were tested. In the first step, neutrons having undergone thermal diffuse scattering (TDS) in the internal volume were eliminated by the recently developed tail suppression method (Agamalian, Wignall & Triolo, 1997). With this modification an additional suppression of the wings of the rocking curve of about one order of magnitude was achieved. The first experiments in this field were done in Wien, at the TRIGA Mark II reactor. The crystal set which is used here are two triple-bounce Si [331] channel cut crystals with a full width at half-maximum (FWHM) of 0.51" (3.3 µrad). By inserting cadmium in the long wall, an additional suppression of the wings of the rocking curve of about one order of magnitude was achieved. These two curves are shown in Fig. 2.

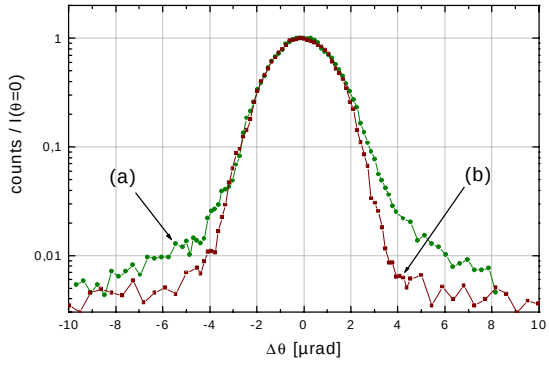

Figure 2

Rocking curves of the triple bounce DCD: (*a*) before cutting, (*b*) after cutting.

The main difference between neutrons and X-rays is the much smaller absorption of silicon for neutrons. Therefore, a component of the incoming neutron beam propagates inside the crystal and contaminates the tail of the rocking curve. After this experiment, the crystal sets for the instrument S18 at ILL in Grenoble and for DKD in Jülich were adapted the same way. The elimination of this parasitic intensity was the first step to shift from the Ewald to the Darwin case. To understand the difference between these two cases better, Fig. 3 illustrates the diffraction process in the case of neutrons.

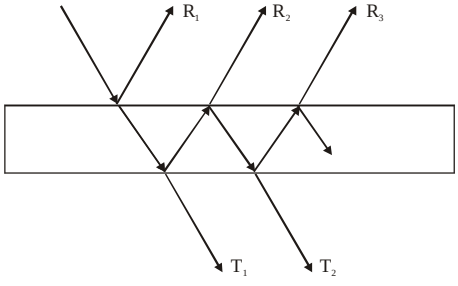

Figure 3

Illustration of the diffraction process for non absorbing crystals.

As shown in Fig. 3, the total reflectivity of a non-absorbing crystal is given by

$$R(y)=\sum_{n=1}^{\infty}R_n(y)$$

$$=R_{\rm D}(y)+\left(1-R_{\rm D}(y)\right)^2R_{\rm D}(y)\left(1+R_{\rm D}^2(y)+R_{\rm D}^4(y)+\ldots\right) \qquad (4)$$

$$=\frac{2R_{\rm D}(y)}{1+R_{\rm D}(y)}$$

where R_1 corresponds to the Darwin formula, the intensity of the transmitted beam through the rear surface, T_1, is given by $(1\text{-}R_{\rm D})^2$. The beam reflected at the rear surface propagates through the crystal, and its reflectivity R_2 is given by $(1\text{-}R_{\rm D})^2R_{\rm D}$. It can also be shown that this equation is equivalent to the Ewald formula. Then, the following relation

$$R_{\rm E}(y)=\frac{2R_{\rm D}(y)}{1+R_{\rm D}(y)} \qquad (5)$$

is obtained between the Darwin and the Ewald formula. The total intensity of the transmitted beam is given by

$$T(y)=\sum_{n=1}^{\infty}T(y)=\frac{1-R_{\rm D}(y)}{1+R_{\rm D}(y)}. \qquad (6)$$

For the wings of a rocking curve (when $R_{\rm D}(y) \ll 1$), the contributions of the front reflection (R_1) and the first back reflection are equal. The higher-order terms do not contribute significantly to the reflection. To measure this effect, the following experiment was performed at DKD in Jülich. Single crystals of Si [111] were prepared to study the influence of the backside reflection. For this purpose, three different sets were tested. One was a normal 0.5 cm thick pair, the second pair was from the same thickness but with a rough surface, and the last set was 1.5 cm thick. The rough surface of the second pair should guarantee that no backside reflection is possible. To have a second option, the 1.5 cm thick pair can be used with an aperture, so that there is also no backside reflection possible. Fig. 4 shows the thick crystal with a cadmium aperture.

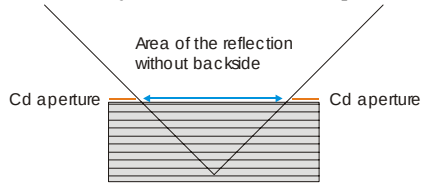

Figure 4

Si [111] crystal without backside reflection.

The crystals were used at a Bragg angle of 45°, so that the wavelength after the monochromator crystal was 4.434 Å. The different experiments showed that the pair with the rough surface was destroyed during the production process. This pair had a very bad reflectivity. The normal pair and the thick one had a very good performance. The best reflectivity was achieved with the thick pair and the cadmium aperture. With this set-up, only planes inside the crystal can contribute to the reflectivity. The backside reflection is not possible for geometric reasons. The different rocking curves measured in Jülich are shown in Fig. 5.

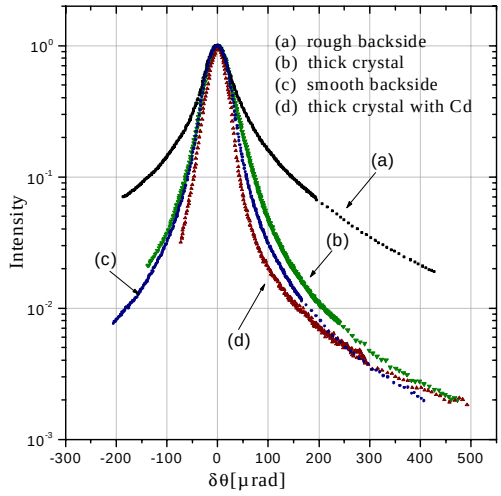

Figure 5

Comparison of the reflectivity for different crystal designs.

To understand the difference between these concepts better, it is important to take a closer look at the term which contributes to the backside reflection. The second term in equation (4), $(1\text{-}R_D)^2R_D$, is the term which corresponds to the backside reflection. This term, together with the neutrons that underwent TDS, is the main difference between the Darwin and the Ewald case. Fig. 6 shows this term before the convolution.

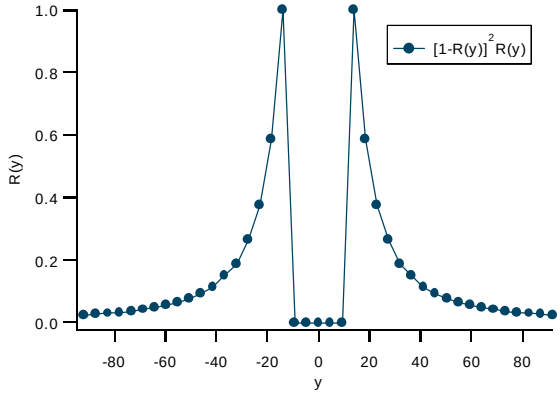

Figure 6

Contribution of the backside to the reflectivity.

The aim was to develop a new crystal design, which has no backside reflection and no background from TDS. To optimise the reflectivity of the crystals, the following steps were taken:

Because the crystals are to be used on a cold source (PSI), with a wavelength of 4.4 Å, the reflection plane [111] was chosen. To reduce the effect of the backside without reducing the area of the incoming beam, a triangular design of the crystals was chosen. With the insertion of a Cd strip between the first and the third plate, the effect of TDS should be eliminated.

Fig. 7 shows the new concept for the perfect crystals.

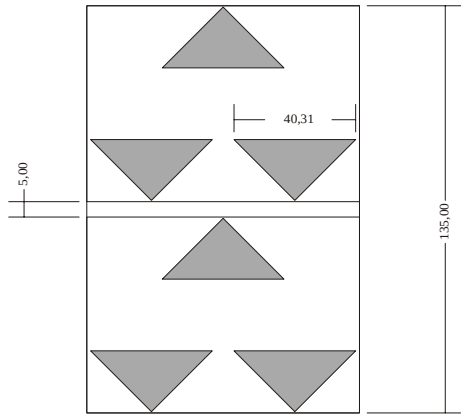

Figure 7

New design for triangular silicon crystals (all parameters in mm).

The triangular design has the advantage that the backside reflection is avoided without reducing the beam diameter. The crystals were cut and afterwards etched in the laboratories of the Atominstitut. For the etching process, a mixture of hydrofluoric acid and nitric acid is used. These two acids are mixed in a ratio of HNO_3:HF => 20:1. During the etching process, the hydrofluoric acid is dissipated, therefore it is necessary to substitute 1 ml of HF for $2x10^{-2}$ mg of weight loss. During the etching process, 8910 mg of silicon were etched from the triple bounce crystals, and around 3000 mg from the single bounce crystals. Because of the cutting process for the two triple bounce crystals, four single bounce crystals were also produced. The depth of the etching process was around 145 μm for the triple bounce, and around 100 μm for the single bounce crystals. With these crystals, a Bonse-Hart set-up was implemented at the instrument TOPSI (Clemens, 2001) at PSI. TOPSI is a two-axis diffractometer, mainly used for reflectometry and simple crystallographic tasks. Therefore, it is not so well adapted to the needs of a DCD. One of the main problems is the high background which may be due to epithermal and fast neutrons from the spallation source. The best results at PSI were reached with a double triple bounce scheme. The results with and without cadmium between the first and the third crystal are shown in Fig. 8.

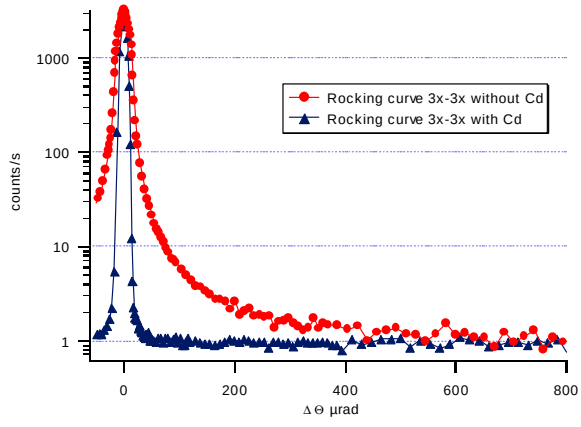

Figure 8

Rocking curve with and without cadmium insert.

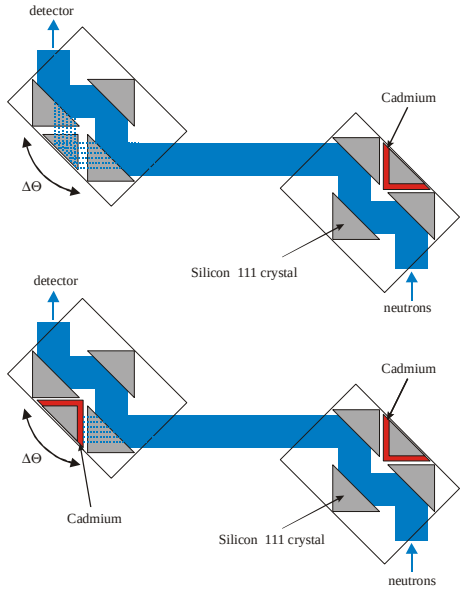

Figure 9

Experimental set-up.

The main difference between these two set-ups is the TDS of the neutrons, and the possibility to allow a single backside reflection from the analyser crystal. This backside reflection corresponds to the term $(1\text{-}R_D)^2R_D$, which was shown in Fig. 6. The influence of this term was measured with the following set-up. With a cadmium strip in front of the second crystal, only neutrons which are reflected on the backside of the crystal are able to reach the detector.

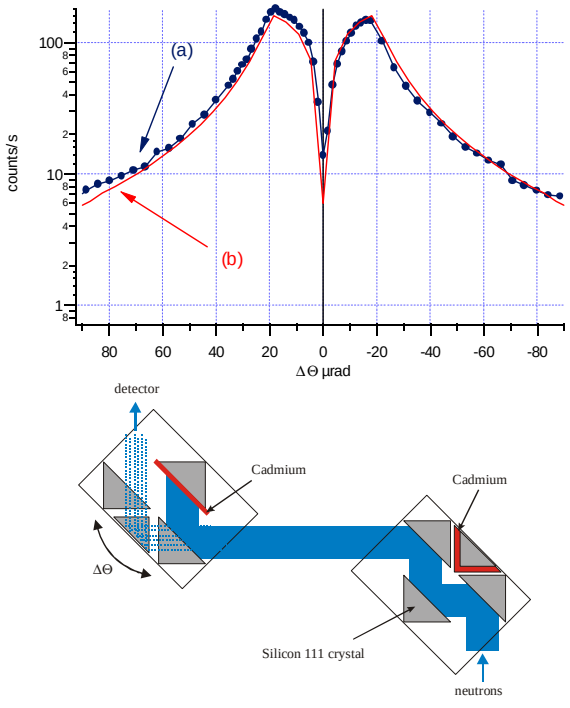

Figure 10

Experimental set-up and results: (*a*) measured curve with second reflection covered with Cd, (*b*) calculated curve.

The curve (b) was calculated from equation (1), with $R_1=R_D$ and $R_2=(1\text{-}R_D)^2R_D$. Fig. 10 shows very clearly the effect of the backside reflection. In the Ewald case, the contribution of the parasitic intensity in the tails of the rocking curve is much higher than in the Darwin case. It is therefore necessary to reduce this background to have a better signal-to-background ratio. Because of the high background at the instrument TOPSI, it was decided to test the same set-up at ILL. Because of the [111] orientation of the crystals, the set-up could not be tested at the S18 instrument (Hainbuchner *et al.*, 2000). The combined interferometry and USANS instrument S18 is located at the thermal guide H25. Therefore, the crystal set was moved to the cold guide H53, and the set-up was installed at the instrument ADAM (Schreyer, 1998). ADAM (advanced diffractometer for the analysis of material) is a reflectometer which provides high flux by use of a focusing monochromator. Similar to TOPSI, ADAM is not well equipped for a DCD set-up, but because of the higher intensity and the lower background, a better signal-to-background ratio was achieved. Fig. 11 shows the result.

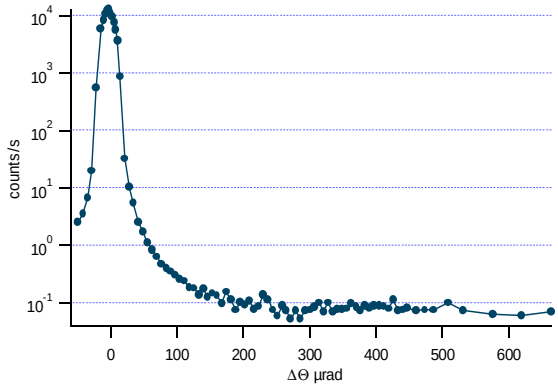

Figure 11

Rocking curve at the instrument ADAM.

4. Summary

To compare the different instruments, it is necessary to change from the scattering angle to the scattering vector *Q*. With this change the different wavelengths of the instruments are no longer relevant. Table 1 and Fig. 12 show the different parameters of the instrument in Wien (KWS), PSI (TOPSI) and at the ILL (S18 and ADAM). At the instrument S18, the crystals with triangular design were not tested, but there the crystals are adapted to the recently developed tail suppression method (Agamalian, Wignall & Triolo, 1997).

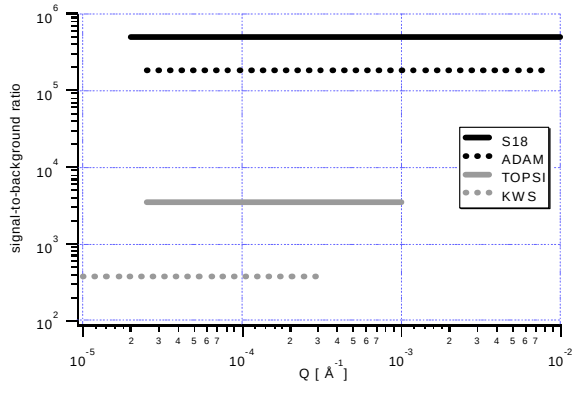

Figure 12

Comparison of the different instruments.

Table 1

Instrument parameters for various USANS DCDs

Instrument	Signal-to-background	Q-resolution [Å-1]	Size range [µm]
KWS	$3.8x10^{2}$	$1x10^{-5}$-$3x10^{-4}$	64-2
TOPSI	$3.5x10^{3}$	$2.5x10^{-5}$-10^{-3}	25-0.6
ADAM	$1.84x10^{5}$	$2.5x10^{-5}$-$8x10^{-3}$	25-0.078
S 18	$5x10^{5}$	$2x10^{-5}$-10^{-2}	32-0.06

As Fig.12 and Table 1 show, the best performance is available at S18, even though there are no crystals with the triangular design. Changing the crystals is not easy, because the monochromator crystal is directly placed in the neutron guide, and every change at the set-up requires an opening of the guide. It is planned to change the crystals in the summer of 2003 when the reactor will be shut down for a longer period. It is also possible to change from the presently used [220] crystals to a [331] set-up. The different measurements have shown that the new design is superior to the parallel plain design. With the triangular design, it is possible to reduce the effect of the backside reflectivity, and with the Cd strip betw een the long wall, the neutrons having undergone TDS are absorbed. Together with newly developed software tools, a strong neutron source and a good crystal design, it is possible to reach the *Q*-range of the SANS region. This may be an attractive option to be incorporated in standard SANS instruments.

The author would like to thank all the colleagues at the different sources around Europe for the beam time and the support during the experiments, especially A. Furrer at PSI, M. Heiderich in Jülich and R. Loidl in Grenoble.

References

Agamalian, M., Wignall, D. G. & Triolo, R. (1997). *J. Appl. Cryst.* **30**, 345-352.
Agamalian, M., Christen, D. K., Drews, A. R., Glinka, C. J., Matsuoka. H. & Wignall, G. D. (1998). *J. Appl. Cryst.* **31**, 235-240.
Bonse, U. & Hart, M. (1965). *Appl. Phys. Lett.* **7**, 238-240.
Clemens, D. (2001). *PSI*, http://sinq.web.psi.ch/sinq/instr/topsi.html.
Darwin, C. G. (1914). *Phil. Mag.* **27**, 675-687.
Ewald, P. P. (1917). *Ann. Phys. (Leipzig)*, **54**, 557-563.
Hainbuchner, M., Villa, M., Kroupa, G., Bruckner, G., Baron, M., Amenitsch, H., Seidl, E., & Rauch, H. (2000). *J. Appl. Cryst.* **33**, 851-854.
Rauch, H., & Petrascheck, D., (1978). *Neutron Diffraction*, edited by H. Dachs, Chapter 9. Berlin: Springer Verlag.
Schreyer, A., Siebrecht, R., Englisch, U., Pietsch, U., & Zabel, H. (1998). *Physica B*, **248**, 349-354.
Takahashi, T., & Hashimoto, M., (1995). *Phys. Lett. A.*, **200**, 73-75.
Zachariasen, W.H., (1967). *Theory of X-Ray Diffraction in Crystals*. New York: Dover.

 Received 29 August 2002 • Accepted 2 January 2003